Analysis of d-core excitons and interband transitions in synchrotron-radiation reflectance spectra of $Cd_{1-x}Mn_xTe$ and $Cd_{1-x}Zn_xTe$ within the energy range from 11 to 20 eV

M. Krause and H.-E. Gumlich
Institut für Festkörperphysik, Technische Universität Berlin, Hardenbergstrasse 36, D-1000 Berlin 12, Federal Republic of Germany

U. Becker
Institut für Strahlungs- und Kernphysik, Technische Universität Berlin, Hardenbergstrasse 36, D-1000 Berlin 12, Federal Republic of Germany

(Received 18 March 1987)

Both Te $5s$-derived interband transitions and the excitations of Cd $4d$ and Zn $3d$ upper core states were studied in $Cd_{1-x}Mn_xTe$ and $Cd_{1-x}Zn_xTe$, respectively. Reflection experiments using synchrotron radiation were performed at $T=115$ K and at room temperature. In $Cd_{1-x}Mn_xTe$ we found new assignments of some spectral lines to interband transitions and core excitons, respectively. In $Cd_{1-x}Zn_xTe$ we have observed a distinct asymmetry in the line shapes of transitions originating from the zinc ions. Based on the model of Fano resonances, these lines are interpreted as resonances of the Zn $3d$ core excitons which decay into the quasicontinuum of the conduction band near the Γ point.

I. INTRODUCTION

The electronic band structure of the semimagnetic semiconductors $Cd_{1-x}Mn_xTe$ and the diamagnetic mixed crystals $Cd_{1-x}Zn_xTe$ depends differently on the composition parameter x.[1-6] This difference is interesting because zinc and manganese have approximately the same ionic radius; however, they show different magnetic behavior. Both crystallize in the zinc-blende structure (space group $F43m$).

The purpose of this paper is to analyze the electronic structure of these materials in the energetic range of the upper d-core levels and the Te $5s$-derived valence-band states. The investigation was performed by reflectance spectroscopy using synchrotron radiation in the range 11–20 eV [Berliner Elektronenspeicherring für Synchrotronstrahlung (BESSY), Berlin]. This method is a useful tool for our problem which is complementary to photoelectron spectroscopy in some ways because unoccupied states as well as occupied states can be studied. As a result of our measurements, some new assignments can be given to spectral lines, where both optical transitions between electronic band states and the excitation of core excitons are taken into account. In addition, interference effects between discrete levels and continua (Fano resonances) are discussed.

Usually, one has to consider the spectrum of the imaginary part of the dielectric function (ε_2) in order to discuss the questions of transition probabilities. However, the values of the reflection coefficient of CdTe and ZnTe are about 5% in the energy range which is considered in this paper.[5] In this case the difference of the peak positions and the line shapes between the reflection spectrum and the imaginary part of the dielectric function becomes small compared to the linewidth.[5] We thus could relate the transitions between the different electronic states directly to the reflection spectrum.

Reflection experiments at room temperature of pure CdTe and ZnTe in the upper energy range were previously reported by Cardona and Greenaway[7] and very recently by Kisiel *et al.*,[8] and at both 300 and 77 K by Freeouf.[9] All these authors assigned the line structure in the energy range 11–15 eV to the Cd $4d$ and Zn $3d$ states, respectively. In this framework, Kisiel *et al.* explain for the first time some fine structure of the reflection spectra due to core excitons.

Reflection spectra of $Cd_{1-x}Mn_xTe$ with $x=0.3$ at room temperature are given by Kendelewicz[10] and also very recently by Kisiel *et al.*[11] In our study, a comparison of the reflection spectra of $Cd_{1-x}Mn_xTe$ ($x=0$ to 0.65) and $Cd_{1-x}Zn_xTe$ ($x=0$ to 0.94), mainly at low temperature ($T=115$ K) is presented together with an analysis of the electronic structure.

The discussion of fine structure in the case of $Cd_{1-x}Mn_xTe$ is restricted to very low concentration x, because of the enlargement of lines due to the interaction of Mn spin-down states in the conduction band.[1,3,6] However, the analysis of the fine structure of $Cd_{1-x}Zn_xTe$ is possible for the whole concentration range. In detail, interband transitions from the Te $5s$ states into the conduction band and core-level excitons due to the excitation of Cd $4d$ states into conduction band states could be assigned for $Cd_{1-x}Mn_xTe$. The dependence of the intensity of some spectral lines upon the concentration x results in assignments different from the assignments given by Kisiel *et al.*[8]

In $Cd_{1-x}Zn_xTe$ we observed two distinct reflection peaks which obviously are connected to Zn $3d$ states. Because of their asymmetric line shapes they could not be analyzed as isolated excitonic transitions, but they are assigned to Fano resonances of core-level excitons interacting with the quasicontinuum of the conduction band near

the Γ point. One of these lines shows a concentration dependence of its asymmetric behavior in accordance with the shift of the fundamental gap as a function of the zinc concentration.

Until now such Fano resonances due to Coulomb interaction between bound states and the quasicontinuum of the conduction bands have been observed in solids in the infrared range by absorption spectroscopy and photoconductivity,[12] and with absorption and reflectance spectroscopy in the visible range.[13,14] In the present paper we demonstrate for the first time that also core excitons in the VUV energy range can lead to asymmetric Fano resonances and that the strength of interference may depend on the energy difference between the bound state and the conduction-band minimum.

The assignment of the interband transitions and the excitonic transitions and resonances is based on calculations of the electronic band structure. These calculations were carried out by Chelikowsky and Cohen[15] for CdTe and by Walter, Cohen, Petroff, and Balkanski[16] for ZnTe using an empirical pseudopotential method. Since these calculations neglect the $4d$ states of Cd and the $3d$ states of Zn, respectively, the experimental results from ultraviolet photoemission spectroscopy (UPS) and x-ray photoemission spectroscopy (XPS) data[2,17] are also considered in the band-structure plots.

The present paper is organized as follows. Section II gives a brief overview of the experimental conditions. The experimental results and the assignments are explained for $Cd_{1-x}Mn_xTe$ in Sec. III. The experimental findings and their interpretations as Fano resonances for $Cd_{1-x}Zn_xTe$ are given in Sec. IV. In Sec. V our conclusions are summarized.

II. EXPERIMENT

The reflection experiments were carried out at the BESSY on the 1m-normal-incidence monochromator. The radiation behind the monochromator was focused to the sample with an incident angle of 9°. This implies that the experiments were done within the normal-incidence range; we were not concerned with the polarization of the radiation.

The crystals were cleaved in air, giving monocrystalline (110) surfaces with a size between 4 and 25 mm^2, and were mounted in a UHV chamber. They were heated to 200–250 °C in order to clean the surfaces *in situ*. The pressure during the experiments was $\lesssim 3\times10^{-9}$ mbar. Thus we are sure that surface contaminations did not result in interference effects at the surface of the sample. The samples were mounted on a manipulator which was rotatable in two axes and connected with a liquid-nitrogen feedthrough. This allowed us to perform experiments at room temperature and 115 K. The error in the temperature determination is ±5 K.

The electromagnetic radiation was detected using a Channeltron ($\times$919Al, Fa. Valvo) in the pulse counting mode. The high sensitivity of the Channeltron enabled us to use monochromator slits of about 10 μm, yielding an energy resolution of $\Delta E=2$ meV at 12 eV. The reflectivity of the samples was determined by dividing the reflection signal by the apparatus function which was controlled after every experimental period. The optical alignment was not well suited to determine the absolute value of the reflectivity, so that normalized spectra are given in this paper.

Most of the crystals examined were grown in our institute by Dr. A. Krost and H.-J. Broschat using the conventional and high-pressure Bridgman technique. Two samples in the upper-concentration range of $Cd_{1-x}Mn_xTe$ were kindly supplied by Professor Becker and Professor Galatzka. The chemical composition of the surfaces examined was determined by F. Galbert using the microprobe technique. The composition was measured at several points of every surface to avoid incorrect interpretations caused by accidental fluctuations.

III. $Cd_{1-x}Mn_xTe$: RESULTS AND DISCUSSION

At room temperature, the spectra of pure CdTe are in agreement with the findings of Freeouf[9] and Kisiel *et al.*,[8] and with earlier measurements of Cardona and Greenaway.[7] However, our spectra show more fine structure than those of Cardona and Greenaway, due to improved resolution.

As to reflection spectra at low temperatures, only the results of Freeouf obtained on CdTe are available.[9] It should be noted that our results agree well with the findings of Freeouf as far as CdTe is concerned.

Reflection spectra of $Cd_{1-x}Mn_xTe$ at room temperature were published by Kendelewicz.[10] These spectra do not show any fine structure in the energy range considered. Our results obtained with $Cd_{1-x}Mn_xTe$ at room temperature are similar to the results of Kisiel *et al.*[8] aside from the fact that our ratio of different peaks within the spectra differs from the ratio observed by these authors. Our results for $Cd_{1-x}Mn_xTe$ with different concentrations of manganese at low temperature are shown in Fig. 1.

In order to analyze the energy of the spectral lines and their shift and broadening as a function of the temperature and of the composition, the spectra were fit by a sum of Lorentz curves using the fit program MINUIT (CERN). To do this it was necessary to assume two functions which describe the underlying background signal originating from the intensive interband transitions in the lower energy range. The result of this fit procedure for pure CdTe is presented in Fig. 2. As the figure shows, a sum of six Lorentz curves L_1–L_6 fits the observed spectrum quite reasonably.

However, one must still be cautious in interpreting each line as a transition without additional support by other complementary experiments. This is especially true if one is interested in excitonic transitions, which would be relatively sharp. Examples of assignment problems in the decomposition of the dielectric functions are known for semiconductors.[18] Some of the decompositions mentioned by this author involve eight or more Lorentzians, whereas the spectrum in question has only two or three critical points or excitonic structures of interest. Having this point in mind we will explain our proposed assignments, which are summarized in Table I and in the fol-

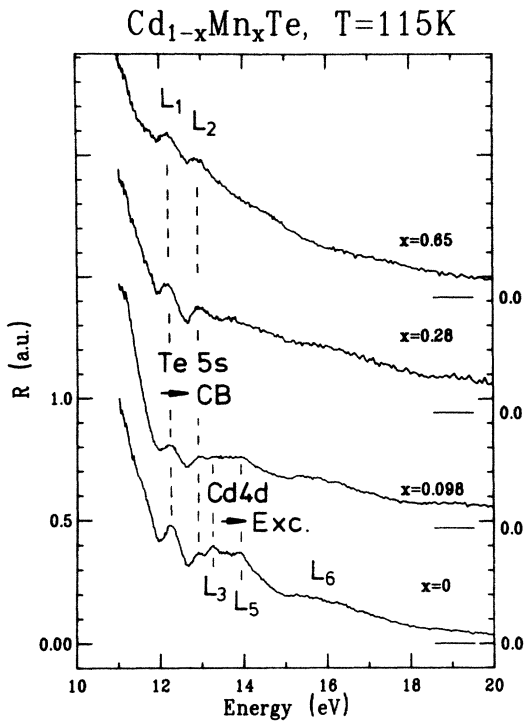

FIG. 1. Normalized reflectivity of different $Cd_{1-x}Mn_xTe$ crystals at 115 K.

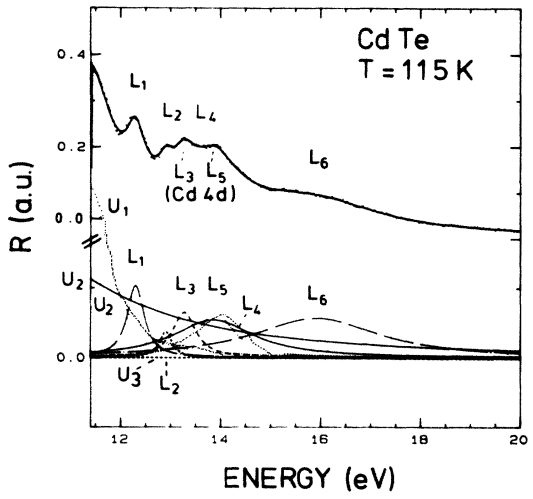

FIG. 2. Line-shape analysis for the reflection spectrum of CdTe at $T=115$ K. The analysis was carried out using Shore-type profiles. The upper curve shows normalized experimental values together with the fitted curves (solid line). The lower curves represent the different components of the fit. L_1 to L_6 are Lorentz curves, U_1 to U_3 are background functions to describe the underlying interband transitions of the lower energy range and a small correction due to the spectral change of the apparatus function U_3.

lowing in more detail. These assignments are based on the following considerations:

(1) Interband transitions take place between the Te $5s$-derived valence bands and the conduction bands. The critical points, where the valence and conduction bands have the same slope, lead to maxima in the combined density of states at the L, X, and Γ points and along the symmetry line Σ of the Brillouin zone.

(2) The Cd $4d$ core levels have an energy of 10.00 eV ($4d_{5/2}$) and 10.65 eV ($4d_{3/2}$) below the valence-band maximum.[2] Transitions between the Cd $4d$ levels and conduction-band states are dipole allowed at the X and L points, but not at the Γ point.

(3) Core-level excitons result from an attractive interaction between the excited electron and the core hole.

(4) Intervalley coupling takes place between the minima of the conduction band.

In Table I we give in addition the half-width of the fitted Lorentz lines and the difference in energy between the experimental value of the maximum and the critical point energy resulting from the band-structure calculation of Chelikowsky and Cohen[15] (see Fig. 3).

In our reflection spectra the maxima L_1 and L_2 are the only lines which can be observed from zero up to high manganese concentrations with similar intensity (Fig. 1). So we conclude that these maxima are probably not due to Cd-based transitions which should disappear with decreasing Cd concentration as shown by other Cd $4d$ transitions. We suggest that these lines are mainly derived from Te $5s$ band transitions to the lowest conduction band at the L point (line L_1) and the X point (line L_2). The assignment of the broad line of L_4 is difficult. We as-

TABLE I. Energy and linewidth of the observed reflection maxima in CdTe at $T=115$ K and the assigned transitions into conduction-band and core-exciton states. The critical-point energies are deduced from the band-structure calculation of Chelikowsky and Cohen (Ref. 15). The binding energy of the core excitons are calculated from the difference in energy between the critical-point energy for the Cd $4d\rightarrow$conduction-band transitions and the reflection peak energy.

Symbol	Reflection maximum (E_R) (fit value) in eV	Linewidth (FWHM) in eV	Assigned transition	Critical point energy (E_c) in eV	E_c-E_R in eV
L_1	12.30	0.34	$L_6\rightarrow L_6$	12.46	0.16
L_2	12.90	0.30	$X_6\rightarrow X_{6,7}$	13.07	0.17
L_3	13.27	0.56	Cd $d_{5/2}\rightarrow$core exciton	13.7	0.43
L_5	13.90	0.90	Cd $d_{3/2}\rightarrow$core exciton	14.3	0.40
L_4	13.86	1.97	Major contribution of $\Sigma_\pm\rightarrow\Sigma_\pm$ assumed	13.9	0.04
L_6	15.9	3.06	Not yet cleared up		

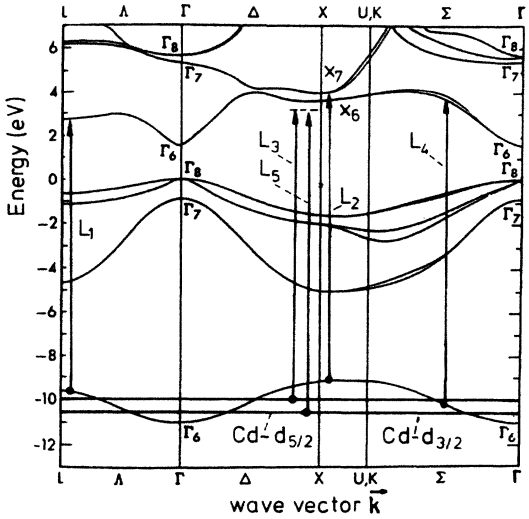

FIG. 3. Electronic-band-structure calculation for CdTe using the empirical pseudopotential method (Chelikowsky and Cohen, Ref. 15). Values for the energy of the Cd 4*d* states below the valence-band maximum are taken from Taniguchi *et al.*, Ref. 1. The arrows describe the assigned transitions into conduction-band states and core excitons, respectively. For the assignments see Table I.

sume that transition $\Sigma_{\pm} \rightarrow \Sigma_{\pm}$ contributes to this line (Fig. 3).

Kisiel *et al.* argue that the transitions within the energy range 11–20 eV are only connected to Cd 4*d* core-level transitions corresponding to the ratio of the degeneracies of the Te 5*s* and Cd 4*d* states.[8] We think that this argument is valid for XP and UP spectra, where the *d* electrons have a much higher cross section than the *s* electrons. However, in our opinion this is not valid for line structures observed in reflection and absorption spectra. As these lines are due to dipole allowed transitions between bandlike states in the initial and final state, their intensity probes the value of the combined density of both states. Such resonantlike transitions can show a much higher transition amplitude for *s* states compared to *d* states at certain photon energies, which is usually not observed in a nonresonant UPS spectrum. The fact that the reflection peaks L_1 and L_2 are clearly detectable even for $Cd_{0.35}Mn_{0.65}Te$ supports our assumption that the contribution to the Te 5*s* states to these lines is important.

The difference in energy between the critical-point energy and the reflection maximum of the lines L_1 and L_2 probably results from an electron-hole interaction which does not lead to Wannier excitons. This kind of interaction plays a dominant role for the energetic location and the line shape of the lower interband transitions (Koster-Slater interaction[19]).

Looking for the assignments of the reflection maxima L_3 and L_5, no critical points within an uncertainty of 0.2 eV can be found for transitions from either the Te 5*s* bands or Cd 4*d* levels to conduction bands. These lines are only observed for small manganese concentrations up to $x = 0.1$ Moreover, they broaden faster with rising temperature than the other lines. The difference in energy ($\Delta E = 0.63$ eV) fits the spin-orbit splitting of the Cd 4*d* states nearly exactly. These facts lead us to the conclusion that the lines L_3 and L_5 are mainly due to transitions from the Cd 4*d* states at the *X* point of the Brillouin zone in combination with the creation of a core exciton. On this assumption the binding energy of the core exciton is found to be $E_b = 0.4$ eV.

The binding energies for core excitons are much larger than the corresponding energies of valence-band excitons. The excitation of core excitons can be observed in many materials for both deeper and lower bound electrons. As two examples we mention the C 1*s* core exciton in diamond[20] and the Ga 3*d* core excitons in GaAs.[21] In the latter example, in addition interband mixing has been observed.

The reasons for the large binding energy of the core excitons are still not unambiguously understood. One argument for explaining the large value is the reduced dielectric screening, which is caused by the relaxation effects of valence electrons in the presence of the core hole. This should lead to virtual electron-hole pairs.[22,23] The second argument is connected to the polarization self-energy of separate electrons and holes in the model of electric polarons.[21,23] The condition for an additional attractive interaction due to this polarization effect is met, when the radius of the polaron is equal or larger than the Bohr radius of the exciton. The quantitative requirements for the attractive interactions depend on the size of the self-energy and the effective masses. As Bassani and Altarelli explained further, the effective-mass theory can still be used for core excitons in semiconductors.[23]

The condition for a polaron-based attractive interaction is certainly not fulfilled at the Γ point of CdTe, but we may expect it at the *X* and *L* point because of the larger effective mass of conduction-band electrons at these points.

Coming to the last points of our arguments concerning the level assignments, we should discuss intervalley coupling, which describes mixing between inequivalent minima of the same conduction band. As a matter of fact, our results cannot give a clear answer to the question of intervalley coupling in $Cd_{1-x}Mn_xTe$. Following the analogy with results obtained with $GaAs_{1-x}P_x$, intervalley coupling is expected to appear in CdTe, because the conduction-band states at the *L* point are located below the *X* point states.[21] In this case, inequivalent minima of the conduction band are mixed together by the core-hole potential, and the core excitons still cannot be assigned to only one critical point.

The transitions which in our opinion give the largest contribution to the observed line structure for CdTe are shown in the electronic-band-structure scheme of CdTe in Fig. 3.

The results obtained with the mixed crystals $Cd_{1-x}Mn_xTe$ show that neither the energy nor the half-width of the reflection peaks L_1 and L_2, which correspond to the Te 5*s* to conduction-band transitions, depend on manganese concentration. This observation is in good accord with the fact that the energy of the Te 5*s*

states in hypothetical MnTe (zinc-blende) is nearly the same as in CdTe.[24]

IV. $Cd_{1-x}Zn_xTe$: RESULTS AND DISCUSSIONS

The normalized reflection spectra of different $Cd_{1-x}Zn_xTe$ crystals are shown in Fig. 4. The distinct reflection peak at 11.67 eV for $Cd_{0.06}Zn_{0.94}Te$ confirms the data of Freeouf for pure ZnTe at 100 K.[9] However, Freeouf finds more fine structure near 13 eV than we do. Also the spectra of Kisiel *et al.*[8] registered at room temperature have more fine structure than our corresponding measurements on $Cd_{0.06}Zn_{0.94}Te$. The authors assign these lines to various Zn $3d$ core transitions and excitons.[8] The earlier measurements of Cardona and Greenaway[7] show less fine structure, as it was mentioned in the above section.

The spin-orbit splitting of the Zn $3d$ states could be expected in the order of 0.5 eV following the values for Zn in the vapor state and elemental solid.[25] Apart from the assignment of reflection maxima to the spin-orbit-split $3d$ states in the paper of Kisiel *et al.*,[8] this splitting was not clearly observed in ZnTe.[25]. Because of the different behavior of the lines S_1 and S_2, which is described below, we do not believe that they indicate the spin-orbit splitting of the $3d_{5/2}$-$d_{3/2}$ states. Nevertheless, the experimental proof of the spin-orbit splitting of the Zn $3d$ states in ZnTe still rests as an open question.

The distinct maxima S_1 and S_2 are clearly connected with the amount of Zn in the mixed crystals. The sharp line structure near S_1 and S_2 is only observed at low temperature, whereas at room temperature only the broad maxima L_1 and L_2 can be detected.

The analysis of more complex spectral features associated with interband transitions was performed recently by modulation spectroscopy as, for example, by numerical differentiation of the reflectance spectra.[21] This method allows in some cases to isolate individual spectral features by fitting line shapes of the derivative spectra. However, derivative line shapes are most suitable for symmetric line shapes in the original spectrum but not for asymmetric line shapes because the differentiation reflects the change of the gradient of a spectral line giving more accurate positions of superimposed Lorentzian lines but obscuring the results from asymmetric lines in the spectrum.

Therefore, in order to examine the shift and the broadening of such lines we tried to fit the spectra not only with Lorentzian line shapes as described in the preceding section but also by more general asymmetric Shore profiles for the lines S_1 and S_2 as shown in Fig. 5 for the crystal $Cd_{0.31}Zn_{0.69}Te$. The physical reasoning of this procedure is based on the model of Fano resonances.

The effect of a Fano resonance occurs when an electronic transition into a bound state is in competition with a transition in a continuum state and an exchange interaction of these states is realized. This leads to a typical asymmetric line shape, which can be described in the case of absorption as follows:[26]

$$k(\varepsilon)=\sigma_0\left[\rho^2\frac{(q+\varepsilon)^2}{1+\varepsilon^2}+1-\rho^2\right],\quad \varepsilon=\frac{E-E_0}{\Gamma/2}, \qquad (1)$$

where ε is the energy displacement from the resonance energy E_0 in units of the resonance half-width. q is the Fano parameter

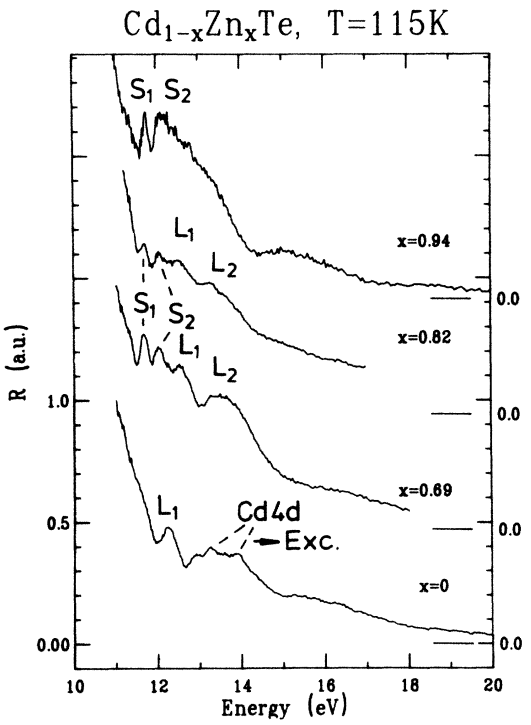

FIG. 4. Normalized reflectivity of different $Cd_{1-x}Zn_xTe$ crystals at 115 K.

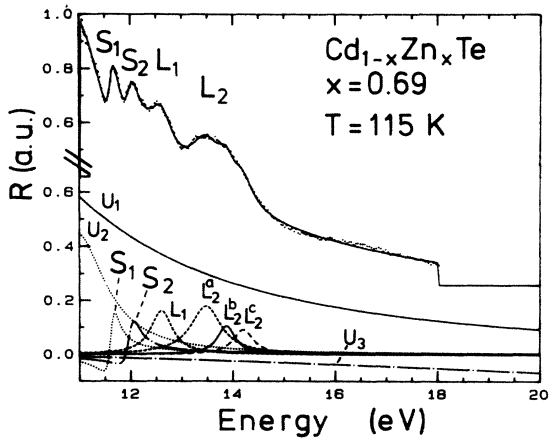

FIG. 5. Line-shape analysis for the reflection spectrum of $Cd_{1-x}Zn_xTe$ ($x=0.69$) at $T=115$ K. The analysis was carried out using Shore-type profiles. S_1 and S_2 are Shore profiles describing the Fano resonances of exciton states with the continuum of the conduction band. L_1 and L_2 [(a)–(c)] are Lorentz curves, which describe the Te $5s$ interband transitions and Cd $3d$ interband-related transitions, respectively. U_1 and U_2 are background functions to describe the underlying interband transitions in the lower energy range whereas U_3 describes a small correction due to the spectral change of the apparatus function.

$$q=\frac{\langle\Phi|\mathbf{r}|g\rangle}{n\sum_{\mu}\langle\Phi|\mathbf{r}|\mu\rangle\langle\mu|\mathbf{r}|g\rangle} \tag{2}$$

and ρ^2 is the strength of interference

$$\rho^2=\frac{\left|\sum_{\mu}\langle\Phi|V|\mu\rangle\langle\mu|\mathbf{r}|g\rangle\right|^2}{\sum_{\mu}\langle\Phi|V|\mu\rangle^2\sum_{\mu}\langle\mu|\mathbf{r}|g\rangle^2}\ . \tag{3}$$

Furthermore, σ_0 is the nonresonant underground, E_0 the resonance Energy, Γ the linewidth [full width at half maximum (FWHM)], $|g\rangle$ the wave function of the ground state, $|\Phi\rangle$ the wave function of the bound state, $|\mu\rangle$ the wave function of one continuum state, numbered with μ, V the operator for the electrostatic interaction, and $\mathbf{r}$ the position vector. Figure 6 (right-hand side) demonstrates the model of Fano resonances.

Although the model of such resonances was developed first for atomic effects by Fano, corresponding effects have also been observed in solids. Whereas in free atoms the energy of continuum states is always above the vacuum level, in a solid, bound states, such as conduction-band states can also form a "continuum." Both types of interactions such as a continuum above the vacuum level[2,27] and with a quasicontinuum below it[12–14] have been observed in solids, respectively.

The left-hand side of Fig. 6 shows the model proposed in the present work in order to explain the asymmetric line shapes in the ZnTe reflection spectra. The transition labeled E creates a core exciton at the X point; the same photon energy may also induce a transition from the Zn $3d$ core level into the conduction band (C). These two final states overlap, leading to an electrostatic interaction. This process is equivalent to the effect of autoionization in free atoms and molecules.

Another approach to the problems of asymmetric line structure could be the discussion of excitonic polaritons (see, e.g., Balslev,[28] Gotthardt, Stahl, and Czajkawski,[29] and Broser and Rosenzweig[30]); however, this will not be considered as an alternative interpretation of our results in the present paper. There is also no need in our opinion to take into account the effect of surface excitons. As Daw, Smith, and McGill found with III-V semiconductors, these effects play a dominant role only in the very first atomic layers near the surface.[31]

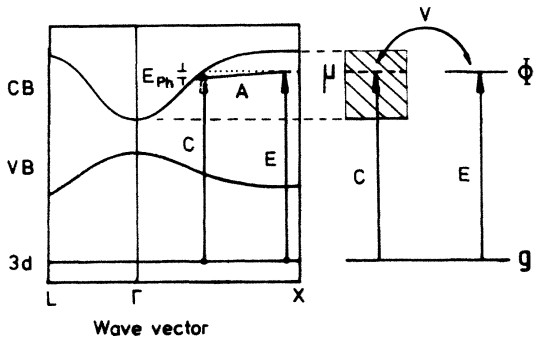

FIG. 6. Model of Fano resonance in a semiconductor. Left-hand side: Plot of the excitation of a core exciton at the X point (E) and its possible autoionizing decay (A) into the continuum of the conduction band. The phonon energy E_{ph} is small compared to the transition energy (not true to scale). Right-hand side: Plot of the levels from the atomic point of view of Fano resonances; g is the ground state, Φ the bound state, and μ one of the continuum states. The double-headed arrow V symbolizes the electrostatic interaction.

To give a quantitative analysis for the Fano resonances it is useful to use the formula for Shore profiles which are more appropriate for a sequence of resonances. For the functions of absorption (k) and refraction (n) they are[32]

$$k(\varepsilon)=\frac{A\varepsilon+B}{1+\varepsilon^2}+C_1,\quad \varepsilon=\frac{E-E_0}{\Gamma/2} \tag{4}$$

$$n(\varepsilon)-1=\frac{A-B\varepsilon}{1+\varepsilon^2}+C_2\ , \tag{5}$$

with A the amplitude of the asymmetric part, B the amplitude of the symmetric part, C_1,C_2 the amplitudes of background, E_0 the resonance energy, and Γ the resonance half-width (FWHM). With knowledge of the parameters A and B, and the magnitude of the underground C_1, the Fano parameters can be evaluated [using Eqs. (1) and (4)]:

$$q=\frac{B\pm(B^2+A^2)^{1/2}}{A}\ , \tag{6}$$

$$\rho^2=\frac{A}{2qC_1}\ . \tag{7}$$

Since the formulas (4) and (5) allow a simple calculation of the optical functions for absorption (k), refraction (n), reflectivity (R) and the imaginary part of the dielectric function (ε_2), it is possible to verify that in the case of small reflectivities of about 5% the asymmetric line shapes of the spectra of R and ε_2 are nearly equivalent. In this way the Shore and Fano parameters obtained by the evaluation of reflection spectra can be applied to the ε_2 spectrum, which is proportional to the transition probability. One should keep in mind that the difference between the Fano parameters q obtained from an ε_2 spectrum on the one hand and from reflection spectra on the other hand for the same transition is still about 20%. Nevertheless, this method allows us to discuss the trends of asymmetric line shapes in $Cd_{1-x}Zn_xTe$.

Table II displays the parameter values of the Shore and Fano line shapes of the reflection peaks S_1 and S_2 for different $Cd_{1-x}Zn_xTe$ crystals. The values of the Fano parameter q and the strength of interference ρ^2 demonstrate that the line S_1 is clearly asymmetric for $x=0.69$ but is nearly pure Lorentzian for the crystal with $x=0.94$. On the other hand, the parameters of the line S_2 indicate that this transition shows an asymmetric behavior which does not depend on the composition parameter within the limits of errors.

This leads us to the conclusion that the asymmetric line S_2 is formed by the creation of a Zn $3d$ core exciton at the X point which is in competition with the Zn $3d$ to conduction-band transitions near the Γ point.

The experimental value for the energy of the Zn $3d$ states in ZnTe is given by Ley as $\Delta E=9.84$ eV below the valence-band maximum.[17] As Himpsel, Eastman, Koch,

TABLE II. Parameter of the observed Fano resonances in different $Cd_{1-x}Zn_xTe$ crystals evaluated from reflection measurements at $T=115$ K. The spectra were analyzed using Shore-type profiles. These fits delivered the resonance energy E_0, the resonance half-width Γ, and the Shore parameters A and B [Eqs. (4) and (5)], which are directly related to the Fano parameter q and the strength of the interference ρ^2 [using Eqs. (6) and (7)].

Parameter	$x=0.69$	$x=0.82$	$x=0.94$
	Line S_1: energy shift $dE/dx=0.4$ eV		
E_0 (eV)	11.62	11.68	11.67
Γ (eV)	0.20	0.20	0.17
A	0.20	0.080	0.0022
B	0.09	0.10	0.20
q	1.6	2.8	180
ρ^2	0.94	0.023	1.2×10^{-5}
	Line S_2: energy shift $dE/dx=0.0$ eV		
E_0 (eV)	11.99	11.98	12.02
Γ (eV)	0.27	0.20	0.37
A	0.13	0.088	0.16
B	0.087	0.061	0.15
q	1.9	1.9	2.3
ρ^2	0.051	0.041	0.070

and Williams show for zinc ions in hexagonal and face-centered-cubic crystals, a crystal field splitting and a dispersion of 0.27 eV can be expected.[33] We combined these values with the electronic-band-structure model of ZnTe, which Walter *et al.* obtained on the basis of the empirical pseudopotential method (Fig. 7).[16] The experimental value of the resonance energy of the line S_2 then leads to an excitonic binding energy of $E_b=0.6$ eV. The conclusions concerning the high value of the binding energy for the core excitons are similar to those described above in the case of $Cd_{1-x}Mn_xTe$.

The asymmetric line S_1 is assigned to a core exciton at the L point. When we consider the energy shift of the fundamental band gap in $Cd_{1-x}Zn_xTe$ at the L point[4] and the dispersion of the $3d$ states, it is obvious that in $Cd_{0.31}Zn_{0.69}Te$ the Zn $3d\rightarrow$conduction-band transitions are resonance partners for the excitonic transitions. In $Cd_{0.06}Zn_{0.94}Te$, there is no possible transition into a continuum state, so that the line shape becomes nearly Lorentzian.

The shift of the resonance energy of S_1 in $Cd_{1-x}Zn_xTe$ with increasing composition parameter x is similar in size to the shift of the transition $E_1+\Delta_1$ ($L_6\rightarrow L_6$, interband transition at the L point).[34] This supports the assignment of the line S_1 to Zn $3d$ core excitons at the L point; the binding energy is found to be $E_b=0.6$ eV.

The lines L_1 and L_2 in the $Cd_{1-x}Zn_xTe$ spectra cannot be assigned only to one main interband or core transition (see Fig. 4). The line L_1 probably has its origin in the interband transitions from Te $5s$ to the conduction band at the L point, as is assumed in pure CdTe. This assignment is supported by taking into account the decreasing intensity of this line with increasing concentration of Zn. Within the energy range near the line L_2, there exist

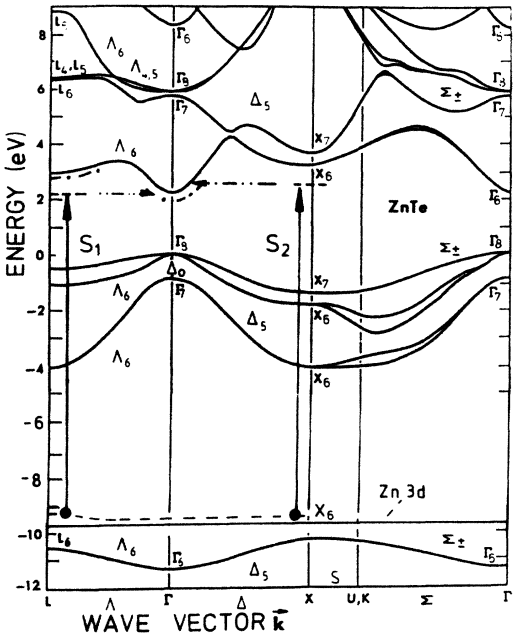

FIG. 7. The observed Fano resonances S_1 and S_2 shown in the plot of the electronic band structure for ZnTe (Walter *et al.*, Ref. 16, using empirical pseudopotential calculations). The value for the energy of the Zn $3d$ state below the valence-band maximum is from Ley *et al.*, Ref. 17. The lower dashed line is the Zn $3d$ band considering the $3d$ dispersion after Himpsel *et al.*, Ref. 33. The dashed line in the upper portion of the figure around the X line is the core-exciton state. $-\cdots\rightarrow$ represents autoionization of the exciton, and $-\cdot-$ the energy of the lowest conduction band for $Cd_{0.3}Zn_{0.7}Te$.

Cd $4d$ excitons as described above, and further transitions from Te $5s$ states into the conduction bands in both CdTe and ZnTe. A discussion of the splitting of the components of line L_2 does not seem to be meaningful at present.

V. SUMMARY

In $Cd_{1-x}Mn_xTe$ and $Cd_{1-x}Zn_xTe$ the transitions from the core states (Zn $3d$ and Cd $4d$, respectively) into conduction bands are superimposed on interband transitions from the Te $5s$ states into conduction-band states. Reflection spectra using synchrotron radiation within the range 11–20 eV are analyzed by taking into account the formation of core excitons and their interaction with the quasicontinuum of the conduction-band states.

By considering the temperature and concentration dependence of the spectral features of the reflectivity, we were able to assign some maxima to core excitons. The binding energy of these excitons could be determined.

The asymmetric shape of the core-exciton lines in $Cd_{1-x}Mn_xTe$ are interpreted as due to Fano resonances between the exciton states and the quasicontinuum of the conduction bands. In one of these cases we found a systematic dependence of the Fano parameter q and the value of the strength of interference upon the concentra-

tion parameter x, which can be explained by the shift of the fundamental band gap with x.

ACKNOWLEDGMENTS

We would like to thank Prof. U. Galatzka (Academy of Sciences, Warsaw), Professor U. Becker (Purdue University, Indiana), Dr. A. Krost [Technische Universität (TU) Berlin], and H.-J. Broschat (TU Berlin) for growing crystals and making them available, Dr. Galbert (TU Berlin) and H. Kerkhoff for expert technical assistance, E. Flach and Ch. Jung for helpful discussions, and Professor A. Kisiel (Krakow) for sending us his papers prior to publication.[8,11] This work was supported by Bundesminister für Forschung und Technologie (BMFT), Bonn, Germany, under Contract No. 05 205 BK and is partly based on a thesis of M. Krause (Ref. 6).

[1]M. Taniguchi, L. Ley, R. L. Johnson, J. Ghijsen, and M. Cardona, Phys. Rev. B **33**, 1206 (1986).

[2]L. Ley, M. Taniguchi, J. Ghijsen, R. L. Johnson, and A. Fujimori, Phys. Rev. B **35**, 2839 (1987).

[3]K. C. Hass, Ph.D. thesis, Harvard University, 1984.

[4]K. Saito, A. Ebina, and T. Takahashi, Solid State Commun. **11**, 841 (1972).

[5]Ch. Jung, E. Flach, H.-E. Gumlich, M. Krause, A. Krost, and U. Becker, in *Proceedings of the International Conference on the Physics of Semiconductors,* Stockholm, 1986, edited by O. Engström (World Scientific, Singapore, 1987).

[6]M. Krause, Dr. rer. nat. thesis, Technische Universität Berlin, Fachbereich Physik, D 83, 1986.

[7]M. Cardona and D. L. Greenaway, Phys. Rev. **131**, 98 (1963).

[8]A. Kisiel, M. Zimnal Starnawska, F. Antonangeli, M. Piacentini, and N. Zema, Nuovo Cimento **8**, 436 (1986).

[9]J. L. Freeouf, Phys. Rev. B **7**, 3810 (1973).

[10]T. Kendelewicz, J. Phys. C **14**, L407 (1981).

[11]A. Kisiel, J. Oleszkiewicz, A. Rodzik, F. Antonangeli, M. Piacentini, N. Zema, A. Balzarotti, and A. Mycielski, Acta Phys. Pol. (to be published).

[12]E. Janzén, G. Grossmann, R. Stedman, and H. G. Grimmeiss, Phys. Rev. B **12**, 8000 (1985).

[13]J. C. Phillips, in *Solid State Physics,* edited by F. Seitz, D. Turnbull, and H. Ehrenreich (Academic, New York, 1966), Vol. 18, p. 137.

[14]M. I. Strashnikova, A. V. Komarov, V. Ya. Reznichenko, V. V. Chernyi, and V. G. Abramishvili, Pis'ma Zh. Eksp. Teor. Fiz. **38**, 18 (1983) [JETP Lett. **38**, 19 (1983)].

[15]J. R. Chelikowsky and M. L. Cohen, Phys. Rev. B **14**, 556 (1976).

[16]J. P. Walter, M. L. Cohen, Y. Petroff, and M. Balkanski, Phys. Rev. B **1**, 2661 (1970).

[17]L. Ley, R. A. Pollak, F. R. McFeely, S. P. Kowalczyk, and D. A. Shirley, Phys. Rev. B **9**, 600 (1974).

[18]W. Verleur, J. Opt. Soc. Am. **58**, 1356 (1968).

[19]Y. Toyozawa, M. Inoue, T. Inoui, M. Okazaki, and E. Hanamura, J. Phys. Soc. Jpn. **22**, 133 (1967); for further details, see M. Cardona, in *Solid State Physics,* Suppl. 11, edited by F. Seitz, D. Turnbull, H. Ehrenreich (Academic, New York, 1969), pp. 41ff.

[20]J. F. Morar, F. J. Himpsel, G. Hollinger, G. Hughes, and J. L. Jordan, Phys. Rev. Lett. **54**, 1960 (1985).

[21]S. M. Kelso, D. E. Aspnes, C. G. Olson, D. W. Lynch, and D. Finn, Phys. Rev. Lett. **45**, 1032 (1980); for the interpretation of the Ga 3*d* core excitons in Ga-V semiconductors, see also H. P. Hjalmarson, H. Büttner, and J. D. Dow, Phys. Rev. B **10**, 5010 (1980).

[22]F. Bassani, Appl. Optics **19**, 4093 (1980).

[23]F. Bassani and M. Altarelli, in *Handbook on Synchrotron Radiation* (North-Holland, Amsterdam, 1963), Vol. 1, pp. 463ff; A. Quattropani, F. Bassani, G. Margaritondo, and G. Tinivella, Nuovo Cimento **51B**, 335 (1979).

[24]K. C. Hass and H. Ehrenreich, J. Vac. Sci. Technol. A **1**, 1678 (1983); for more details see Ref. 3, pp. 8ff, and Ref. 6, p. 91. The electronic structure of the Te 5*s* states seems to be independent of the manganese concentration, whereas the conduction-band states depend on both the variation of the lattice parameters and the interaction between the conduction-band states and the Mn *d* electrons.

[25]$\Delta E = 0.337$ eV for Zn II and $\Delta E = 0.54$ eV for Zn metal, Ref. 17 and $\Delta_{SO} = 0.30$ in ZnTe.

[26]U. Fano and J. W. Cooper, Phys. Rev. B **137**, A1364 (1965); for further details of the parameter interpretation see, e.g., P. H. Kobrin, U. Becker, S. Southworth, C. M. Truesdale, D. W. Lindle, and D. A. Shirley, Phys. Rev. A **26**, 842 (1982).

[27]M. Taniguchi, S. Suga, M. Seki, H. Sakamoto, H. Kanzaki, Y. Akahama, S. Endo, S. Terada, and S. Narita, Solid State Commun. **49**, 867 (1984).

[28]I. Balslev, Solid State Commun. **52**, 351 (1984).

[29]L. Gotthardt, A. Stahl, and G. Czajkowski, J. Phys. C **17**, 4865 (1984).

[30]I. Broser and M. Rosenzweig, Phys. Rev. B **22**, 2000 (1980); for further details see M. Rosenzweig, Dr. rer. nat. thesis, Technische Universität Berlin, Fachbereich Physik, D 83, 1982.

[31]M. S. Daw, D. L. Smith, and T. C. McGill, Solid State Commun. **6**, 449 (1983).

[32]B. W. Shore, J. Opt. Soc. Am. **57**, 881 (1967).

[33]F. J. Himpsel, D. E. Eastman, E. E. Koch, and A. R. Williams, Phys. Rev. B **22**, 4604 (1980).

[34]See Ref. 6, p. 103 (unpublished data), and Ref. 4.